MODELING FLOW CURVES OF HLSA AND IF STEEL IN THE AUSTENITE

José Rubens Gonçalves Carneiro
Pontifical Catholic University of Minas Gerais – PUCMINAS, Belo Horizonte, MG, Brasil
joserub@pucminas.br

Jefferson José Vilela
National Commission of Nuclear Energy – CNEN/CDTN, Belo Horizonte, MG, Brasil
jjv@cdtn.br

Ronaldo Barbosa
Federal University of Minas Gerais - UFMG, Belo Horizonte, MG, Brasil
rbarbosa@demet.ufmg.br

Guilherme Mariz de Barra
Pontifical Catholic University of Minas Gerais – PUCMINAS, Belo Horizonte, MG, Brasil
guiga@pucminas.com.br

Pedro Paiva Brito
Pontifical Catholic University of Minas Gerais – PUCMINAS, Belo Horizonte, MG, Brasil
pedrobrito@pop.com.br

Abstract. *The influence of C, Nb, Nb-B and Ti in flow curves was studied in 8 alloys with controlled chemical composition. The torsion test was used to obtain the flow curves at a strain rate of 0.1, 1, 3 and 10 s^{-1} and temperatures of 1050, 1000, 950, 900 and 850 ºC. All curves and all steels showed one maximum that indicates dynamic recrystallization.*

The flow curve could be divided in three regions: work hardening, recovery and dynamic recrystallization. The interaction between the hardening and smoothing mechanism is dependent on chemical composition and strain. The equations for hot deformation in function of chemical composition were proposed by Sellars (1985) and Medina and Hernandez (1996). A relation between the parameters B_H , C', m_H, B', k', m', e_c and e_p with Z/A showed a higher standard deviation and large fitting errors between the models and experimental data (Medina and Hernandez, 1996). And, a precision methodology has not been developed to obtain yield stress and critical strain yet. These parameters depend on the conditions of strain and austenite chemical composition. The assessment error flow curve between measured and calculated was 4.73 and standard deviation is 3.14.

Keywords*: IF steel, hot rolling, flow curve, HSLA steel*

1. Introduction

The interstitial free steels have been developed in last two decades in order to improve the quality of deep drawing (Hulka, 1991; Butterworth, 1982). The precipitation of carbon and nitrogen with Ti, Nb and Al is changing the schedule rolling. And load rolling is the easiest variable process to measure.

The simulation of flow curve in ideal conditions is the first step for modeling load of rolling (Anderson and Evans, 1996; Rao and Hawbolt, 1992; Baragar 1987, Sellars 1986 and Medina and Hernandez, 1996). The parameters could be classified like the process (strain, rate strain, and temperature) or the materials (size grain, fraction of smoothing or hardening between strains). These models could be represented for Equations (1) and (2) where, the stress is function of strain, strain rate and temperature.

$$s = f(e, \dot{e}, T) \tag{1}$$

$$Z = \dot{e} \exp\left(\frac{Q_{def}}{RT}\right) \text{(Zener and Hollomon, 1944)} \tag{2}$$

Q_{def} is the apparent activation energy for hot deformation, R is the universal constant of gases and T is the absolute temperature. Sellars and Tegart (1966) proposed the following expression for temperature, rate strain, and stress and strain.

$$Z = \dot{e}\exp\left(\frac{Q_{def}}{RT}\right) = A\,\mathrm{senh}(a s_p)^n \quad (3)$$

σ_p is the peak stress. The apparent activation energy for hot deformation is a function of the parameter Z. Work hardening, recovery and dynamic recrystallization could be emerged when the steels are strained in austenite. Hernandez, Medina and Ruiz, 1996 developed a model to predict the whole flow curve for low carbon and HSLA steels, using the Zener-Hollomon parameter, peak stress, peak strain and chemical composition, with temperatures varying from 900 and 1100 °C and strain rate varying from 0.54 to 5.22 s^{-1}. The objectives of this work were:

- to obtain flow curves of IF steels and microalloys (Ti, Ti-Nb and Ti-Nb-B),
- to model stress of IF steels and microalloys (Ti, Ti-Nb and Ti-Nb-B) in function of strain, temperature, strain rate and chemical composition for large strains.

2. Methodology

The chemical compositions of eight alloys that were studied in this work are showed in Table 1. The ingots of alloys weighting 45 kg were cast in a vacuum furnace. They were heated at 1180 °C during three hours. Afterwards, they were forged in billets with cross section area of 30 x 70 mm^2. The specimens were machined parallel to rolling direction. The hot torsion tests were made on a servo-hydraulic machine MTS 880-14 that was equipped with infrared heating system. The specimens were heated at 1200 °C, during a quarter of an hour. After that, they were cooled at the rate of 1°C/s down to the test temperatures (1100, 1050, 1000, 950, 900 or 850 °C). They were tested with strain rates of 0.1, 1, 3 and 10 s^{-1}.

Table 1. Chemical composition of alloys studied in this work, % mass.

Alloy	C (ppm)	Mn	Si	P	S	Al	Ti	Nb	N_2 (ppm)	B (ppm)
1	24	1.70	0.17	0.006	0.002	0.021	0.014	0.110	9	-
2	28	0.15	0.01	0.013	0.009	0.058	0.083	-	38	-
3	89	0.13	0.01	0.008	0.010	0.058	-	-	22	-
4	270	1.70	0.16	0.009	0.003	0.016	0.015	0.048	10	-
5	260	1.70	0.16	0.006	0.003	0.026	0.016	0.110	10	-
6	250	1.66	0.16	0.007	0.003	0.026	0.014	0.110	10	23
7	270	1.69	0.17	0.006	0.002	0.026	0.017	-	9	-
8	4800	0.90	0.21	0.023	0.011	0.012	0.002	0.003	65	-

The data was converted to shear stress (τ) through Equation (4) and shear strain (γ) (Roucoules, 1996).

$$t = \frac{M[3+m+n]}{2pr^3} \quad (4)$$

The “m” and “n” parameters were considered constants 0.17 and 0.13 respective. In this procedure, the uncertainties of stress are ± 5 % (Roucoules, 1996).

The dimensions specimens changed during the test due to larger strains. The change diameter and length was assumed linear. The stress and strain were corrected using the approach developed by Vilela (1999). During the test, a large amount of the total energy was transformed to thermal energy. In this work, correction of temperature due to adiabatic heating was done using the approach developed by Almeida (1996).

3. Results and Discussion

The yield stress can be calculated through solution of differential equation correspondent to the second stage of the hardening curve in function of stress (Cahn, 1957). The solution is:

$$s = q_2(e - e^*) \quad (5)$$

θ_2 is the first order derived stress in relation to strain. ε^* is a constant which value is similar to the strain for the beginning of the second stage. In the second stage of hardening, θ_2 is calculated in the following expression:

$$q_2 = \left(\frac{am}{2p}\right)\left(\frac{bn^*}{3\Lambda_a}\right)^{0,5} \tag{6}$$

Λ_a is a constant equal to 0.0004 cm, n* = 25 and μ is the shear modulus. In the Figure 1, the results of the theoretical rate hardening θ_2 for alloy 5 in function of temperature and different strains rate are showed. The θ_2 values were 143.05, 170.16 and 195.44 MPa for 1050, 950 and 850 °C respectively, with a strain rate $0.1 s^{-1}$.

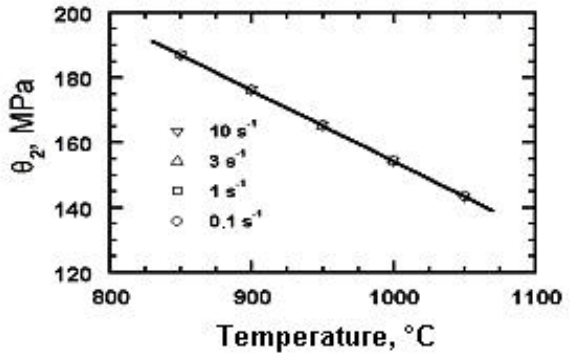

Figure 1. The value of θ_2 in different strain rate in function of temperature, for alloy 5.

The theoretical hardening rate was obtained through derivation flow curve in different temperatures and constant strain rate. The yield stress can be calculated using Equations (5) and (6). The equation that was developed by Cahn (1957) for ε_c can be used in the second stage of flow curve at low temperatures. All flow curves showed decrease in hardening between yield strain and peak strain. This behavior occurs when materials undergo dynamic recrystallization. In the third stage, the hardening rate increased with stress but decreased with temperature (Figure 2).

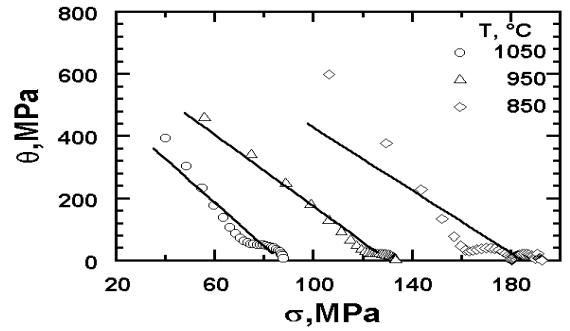

Figure 2. Work hardening rate in function of stress, in different temperatures, for alloy 5, strain rate $0.1 s^{-1}$.

Ryan (1989) divided the curve $\theta \times \sigma$ in three linear segments, where the last segment define critical stress for dynamic recrystallization (σ_{ss}^*) (Figure 3). After critical stress, θ decreases with more intensity due to dynamic recrystallization until peak stress (σ_p), where $\theta = 0$. σ_{ss}^* was obtained through extrapolation of one linear segment until $\theta = 0$ in the second stage. This chart methodology is not reliable. Poliak and Jonas (1996) proposed another method where dynamic recrystallization commenced appearing in the inflection point of the curves $\theta \times \sigma$ or $\ln(\theta) \times \varepsilon$. According to the authors, in this method is not necessary to use extrapolation. In this work, the $\ln(\theta) \times \varepsilon$ curve show oscillations that made the determination of ε_c difficult. The $\ln(\theta) \times \varepsilon$ curve was smoothed using the adjacent averaging method with seven points. Equation (7) shows a linear fit of $\ln(\theta) \times \varepsilon$ curve between strain in the end of second stage and outset of change concavity (Figure 4).

$$s_{\text{recuperação}} = \frac{\exp\left(-a_{ss}e + b_{ss}\right)}{-a_{ss}} + c_{ss} \tag{7}$$

The constant "c_{ss}" was obtained through substitution in the recovery curve (Perdrix, 1982). The determination of a_{ss} and b_{ss} was not precise, because the interval in the $\ln(\theta) \times \varepsilon$ curve used for linear regression was unknown (Figure 4). Also the imprecise measures of ass and b_{ss} effected c_{ss}. However, with this method, ε_c is determined without

extrapolation. The critical stress was the first positive value that was obtained between the flow curve and the curve without dynamic recrystallization (Figure 5). Q_{def}, α and n were calculated using Equations (3) and (8).

$$\left[\frac{\partial \ln(\dot{e})}{\partial \ln \operatorname{senh}(a s_p)}\right]_T \text{ and } \left[\frac{\partial \ln \operatorname{senh}(a s_p)}{\partial(1/T)}\right]_{\dot{e}} \tag{8}$$

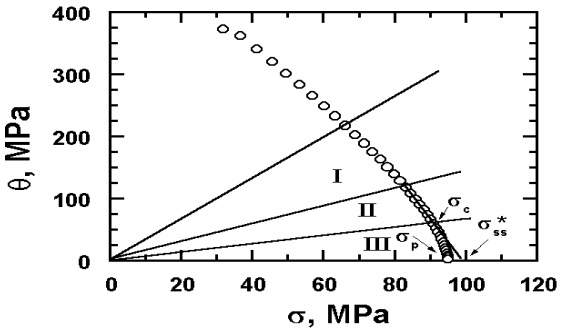

Figure 3. Methodology of Perdrix (1982) to obtain critical strain for alloy 3, temperature 1050 °C and strain rate 1 s^{-1}.

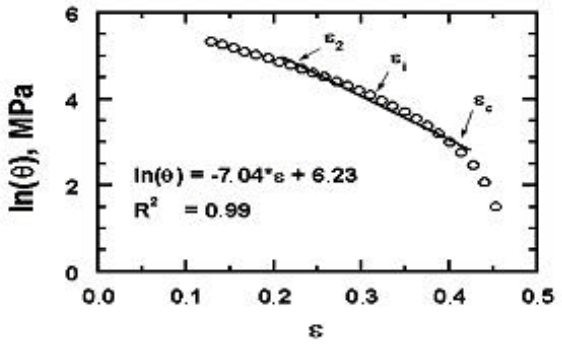

Figure 4. Adjustment of Equation (7) for alloy 3.

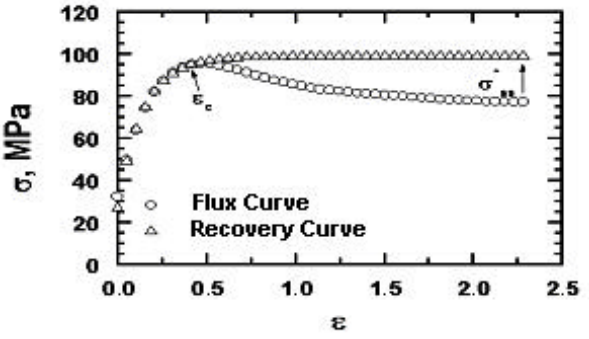

Figure 5. This approach was used to obtain critical stress for alloy 3, temperature 1050 °C and strain rate 1 s^{-1}.

With the activation energy, α and n for studied alloys, the parameter Z could be calculated by Equation (3). Through software it was possible to determine the value of α that allowed for a minimum standard deviation. The results showed that the system did not have only one solution to α and n in Equation (3), which were only mathematical adjustment. With α, n and Q_{def} values, it was possible to determine constant A (Table 2). However, parameter A was not constant for all alloys (Figure 6). Also, "A" was modeled with chemical composition:

$$A\ (s^{-1}) = (12.197 + 65.590(\%\ C) - 49.052\ (\%\ NB))\exp(0.00007076\ Q_{def}) \tag{9}$$

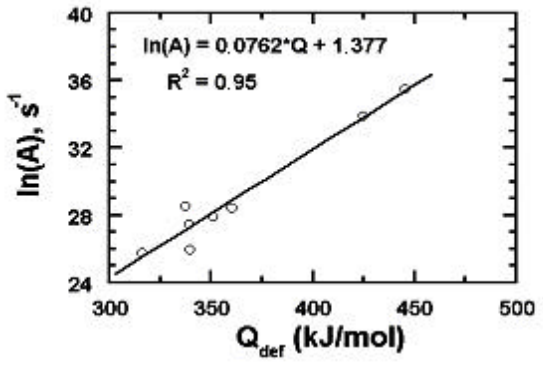

Figure 6. Correlation between coefficient A and activation energy Q_{def} for all alloys.

Q_{def} could be related chemical composition. The Nb in solution was more effective in the increase of activation energy (alloy 1) (Figure 7a) or precipitated like NbTiCN (alloys 4 and 5) (Figure 7b) (Roucoules 1992). The Ti in solution (alloy 2) also produced increase in Q_{def}. The increase was higher in alloy 8, where precipitate potential was smaller (Figure 8). The B also increased Q_{def} (Figure 9), the segregation of BC and BCN in dislocations, boundary grain and subgrain increase the chemical force for nucleation (Roucoules 1992).

Table 2. Values of Q_{def} and ln (A) calculated for averages α and n..

Alloy	α	N	Q_{def} average (J/mol)	Standard Deviation of Q_{def}	ln(A) (s^{-1})
1	0.016	3.89549	339871.47	1670	25.93451
2	0.016	3.89549	351311.50	1709	27.87237
3	0.016	3.89549	316323.04	1546	25.72913
4	0.016	3.89549	360511.05	1776	28.37775
5	0.016	3.89549	425059.53	2077	33.85711
6	0.016	3.89549	445793.83	2186	35.46077
7	0.016	3.89549	339358.11	1475	27.45060
8	0.016	3.89549	337818.54	1855	28.47691

The multiple regression was obtained for values of Q_{def} with chemical composition, that was similar to Medina and Hernandez, 1996.

$$Q_{def} = 285.50\,\%C + 17.52\,\%Mn + 1757.25\,\%Al + 790.48\,\%Nb + 475.87\,\%Ti - 1587.75\,\%N + 11024.7\,\%B - 206.229\,\%Si + 114.911\,\%P + 216.062 \quad (10)$$

Hernandez, Medina and Ruiz, 1996 showed that the difference in the Q_{def} was due to fraction and atomic volume of substitution element solute. The Nb added to alloys 4, 5, and 8 increased the energy activation. The alloys 1 and 5 had almost the same content of Nb and Ti, but energy activation was higher in alloy 5. These results showed that the energy values depended on interstitial in the alloy. The hardening was modified with dynamic precipitate. This work showed that activation energy was depended on the fraction atomic solution. With Q_{def} calculated, the flow curve without dynamic recrystallization could be modeled using Equations (2) and (10).

The parameters B_H, C' and m_H were dependent on the state of strain and chemical composition of austenite. Equation (11) is similar to Avrami's equation (1939) and was used to calculate stress larger that critical stress. However, yield stress was not considered because the experimental measure was not reliable.

$$s_e = B_H\left[1-\exp(-C'e)\right]^{m_H} \quad e \le e_c \quad (11)$$

Equation (12) was used to calculate the flow curve in function of strain. The peak strain and stress, critical stress and strain, stress in the stationary dynamic recovery and in dynamic recrystallization were function of the Z/A parameter for all alloys. Also, the parameters B_H, C', m_H, B', k' and m' were in function of Z/A. Hernandez, Medina and Ruiz (1996) used power and logarithmic equations to relate these parameters with Z/A. In Figures 10 to 16, the relations for each parameter in function of Z/A are showed for alloy 5. Equation (12) was substituted in Equation (13). And flow curves in function of strain were calculated as shown in Figure 17 for a strain rate of 10 s^{-1} and temperatures of 850, 900, 950,

1000 and 1050 °C. Equation (14) was used to calculate the mean error (Rao and Hawbolt, 1992) for alloy 5 that was found to be 3.34 %.

$$\Delta s = B'\left(1-\exp\left[-k'\left(\frac{e-e_c}{e_p}\right)^{m'}\right]\right) \tag{12}$$

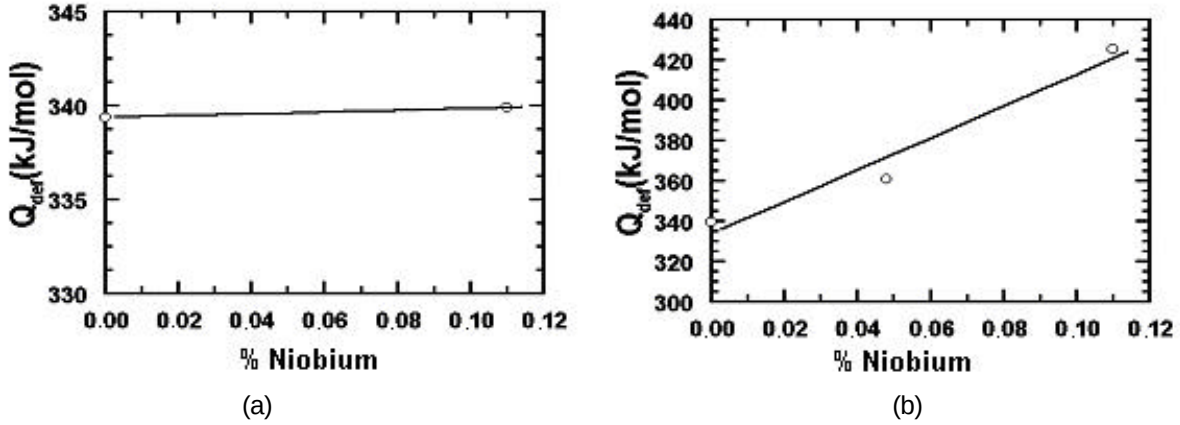

Figure 7. (a) Dependence of Q_{def} with Nb for alloys (C-Mn-Ti-Nb) in solution 1 and 8 (b) in dynamic precipitation 8, 4 and 5.

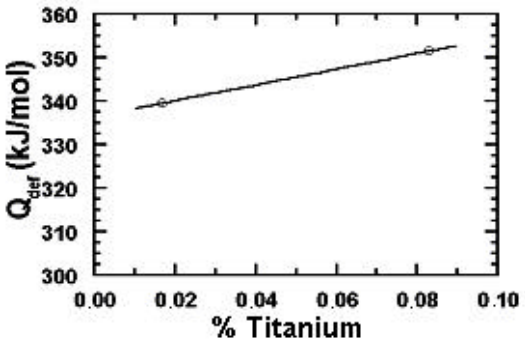

Figure 8. Dependence of Q_{def} with Ti for alloys 7 and 2 (C-Mn-Ti).

$$s = s_e - \Delta s \tag{13}$$

$$Error(\%) = \frac{1}{p}\sum_{1}^{p}\left(\frac{s\ \text{calc} - s\ \text{meas}}{s\ \text{calc}}\right)x100 \tag{14}$$

The parameters m_H and m' were constants in different alloys and strain, according to Sellars (1985) and Vilela (1999). These parameters were proposed as function of strain by Hernandez, Medina and Ruiz (1996), but in their equations, the coefficient of determination was low. The bad adjustment between Z/A and the parameters (C', m_H, k' and m') explained the errors found between the calculated and experimental flow curves. Other authors (Roucoules 1996, Hernandez, Medina and Ruiz, 1996) said the error was caused by the adiabatic heats.

The interaction between work hardening, dynamic recovery, dynamic recrystallization and dynamic precipitation was too complex and influenced by chemical composition and strain. This fact created a bad statistical relation between the parameters B_H, C', m_H, B', k', m', ε_c and ε_p with Z/A, that contributed for increasing the errors in modeling flow curves. With this model, the effect of drag solute in the matrix could be evaluated as well as kinetics of precipitation and dynamic recrystallization.

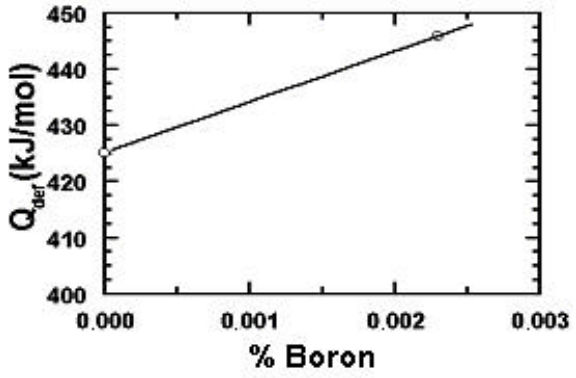

Figure 9. Dependence of Q_{def} with B for alloys 5 and 6.

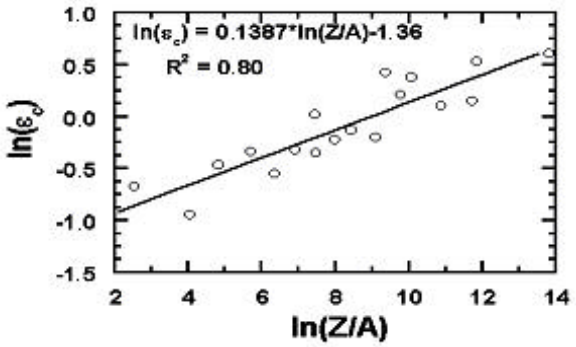

Figure 10. Critical strain in function of parameter Z/A, for alloy 5.

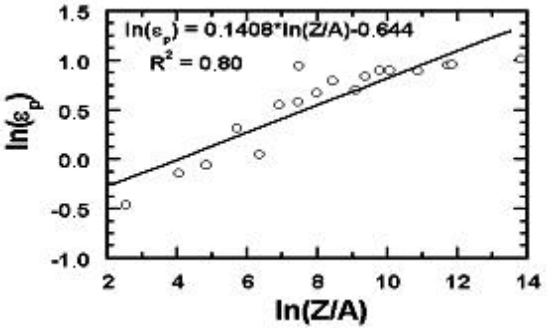

Figure 11. Peak strain in function of parameter Z/A, for alloy 5.

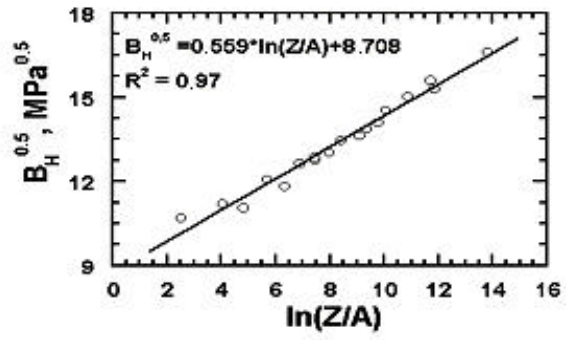

Figure 12. Parameter B_H in function of parameter Z/A, for alloy 5.

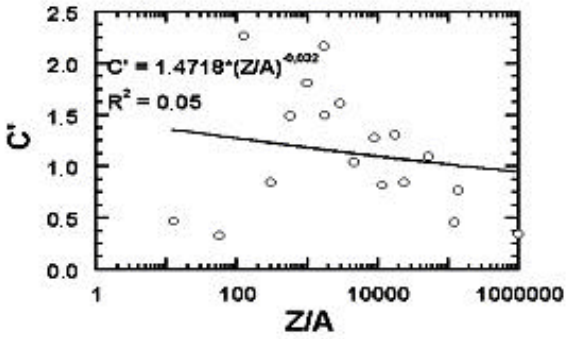

Figure 13. Parameter C' in function of parameter Z/A, for alloy 5.

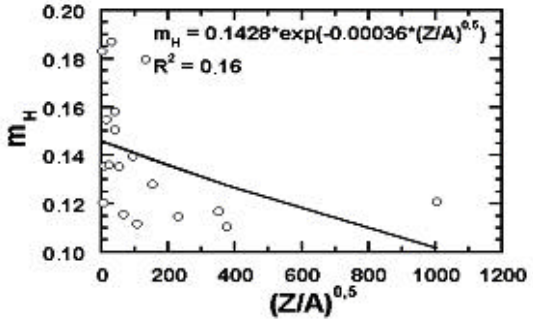

Figure 14. Exponent m_H in function of parameter Z/A, for alloy 5.

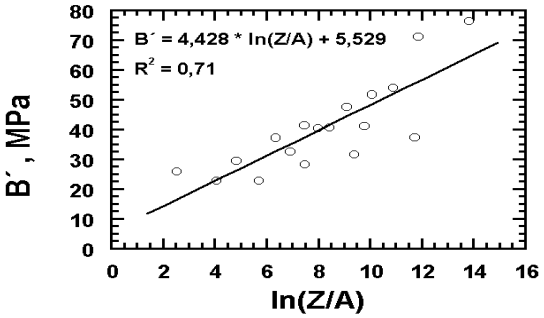

Figure 15. Parameter B' in function of parameter Z/A, for alloy 5.

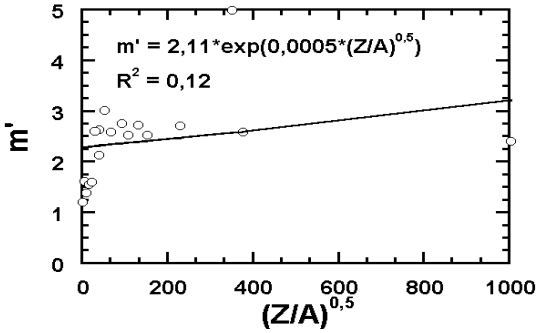

Figure 16. Parameter m' in function of parameter Z/A, for alloy 5.

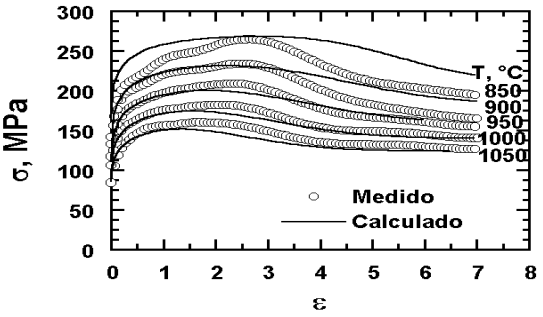

Figure 17. The comparison between flow curve obtained by torsion test measured and calculated using model proposed, for alloy 5, strain rate 10 s^{-1} and temperatures 850, 900, 950, 1000 and 1050 °C.

4. Conclusion

The interaction among work hardening, dynamic recovery, dynamic crystallization and dynamic precipitation was too complex and influenced by chemical composition and strain.

The proposed equations were valid in conditions of the test for studied alloys.

5. Acknowledgements

The authors thank AÇOMINAS.

6. References

ALMEIDA, J. A. Obtenção de Curvas Tensão-Deformação via Ensaio de Torção a Quente em Aços Inoxidáveis Austeníticos ABNT 304 e ABNT 316 a taxas de deformação entre 0.1 e 100 s^{-1}. Belo Horizonte: UFMG, 1996. 121p. Dissertação (Mestrado em Engenharia Metalúrgica e de Minas) - Escola de Engenharia da UFMG, 1996.

ANDERSON, J. G., EVANS, R. W. Modeling Flow Stress Evolution during Elevated Temperature Deformation of Two Low Carbon Steels. Ironmaking and Steelmaking, v. 23, n. 2, p. 130-135, 1996.

AVRAMI, M. Kinetic of Phase Change, I. Journal of Chemical Physics, v. 7, p. 1103-1112, 1939.

BARAGAR, D. L. The High Temperature and High Strain-Rate Behavior of a Plain Carbon and an HSLA Steel. Journal of Mechanical Working Technology, v. 14, p. 295-307, October 1987.

BUTTERWORTH, C. The Future of Interstitial-Free Steels Iron and Steel International, April, p.83-86, 1982.

CAHN, R.W. Mechanical Properties, Middle Temperature-Dependent. New York. Ed. John Wiley & Sons, 1957. 576p.

HERNANDEZ, C. A., MEDINA, S. F., RUIZ J. Modeling Austenite Flow Curves in Low Alloy and Microalloyed Steels. Acta Mater., v. 44, n. 1, p. 155-163, 1996.

HULKA, K. Development Trends in High Strength Structural Steels. In: Processing Microstructure and Properties of Microalloyed and Other Modern High Strength Low Alloy Steels, IN. Procedures Warrendale TMS, 1991, Pittsburgh, p. 177-187.

MEDINA, S. F., HERNANDEZ, C. A. General Expression of the Zener-Hollomon Parameter as a Function of the Chemical of Low Alloy and Microalloyed Steels. Acta Mater., v. 44, n 1, p. 137-148, 1996.

PERDRIX, C. Caracteristiques D'Ecoulement Plastique du Metal Dans les Conditions du TAB a Chaud – Commission des Communantes Europeennes – Rapport Technique des Travaux Effectues Pendent – France - 1982.

POLIAK, E. I., JONAS, J. J. A One-Parameter Approach to Determining the Critical Conditions for the Initiation of Dynamic Recrystallization. Acta Mater., v. 44, n. 1, p. 127-136, 1996.

RAO, K. P., HAWBOLT, E. B. Development of Constitutive Relationships Using Compression Testing of a Medium Carbon Steel. Transactions of the ASME, v. 114, p. 116-122, January 1992.

ROUCOULES, C. Dynamic and Metadynamic Recrystallization in HSLA Steels. Montreal: McGill University, 1992. 269 p. Thesis of Doctorate - McGill University, 1992.

RYAN, N. D. Work hardening, strength, restorative mechanisms, and ductility in the hot working of 300 series stainless steels. Montreal: Concordia University, 1989. 215p. Thesis of Doctorate in Mechanical Engineering, Concordia University, 1989.

SELLARS, C. M. The Kinetics of Softening Processes during Hot Working of Austenite. Czech. J. Phys., v. 35, p. 239-248, 1985.

SELLARS, C. M., McG. TEGART, W. J. M. La Relation entre la Résistance et la Structure dans la Déformation à Chaud. Mémoires Scientifiques Rev. Métallurg, v. 63, n. 9, p. 731-746, 1966.

VILELA, J. J. Modelagem de Curvas de Fluxo para Aços Livres de Intersticiais. Belo Horizonte: UFMG, 1999. 265p. Tese (Doutorado em Engenharia Metalúrgica e de Minas) -Escola de Engenharia da UFMG, 1999.

ZENER, C. H., HOLLOMON, J. H. Effect of Strain Rate Upon Plastic Flow of Steel. Journal of Applied Physics, v. 15, p. 22-32, January 1944.

5. Responsibility notice

The five authors are the only responsible for the printed material included in this paper.